

Max-Planck-Institut  
für Mathematik  
in den Naturwissenschaften  
Leipzig

A mesoscopic model for helical bacterial flagella

by

*Benjamin Friedrich*

Preprint no.: 74

2005





Preprint

# A mesoscopic model for helical bacterial flagella

Benjamin Friedrich<sup>1</sup>

Max-Planck-Institute for Mathematics in the Sciences,  
Inselstraße 22, 04103 Leipzig, Germany

July 2005

Keywords: Lattice-rotation-model, bacterial flagella, polymorphism, multi-state control problem

## Abstract

Filaments of bacterial flagella are perfect tubular stackings polymerized out of just one kind of building block: the flagellin protein. Surprisingly, they do not form straight rods, but exhibit a symmetry-breaking coiling into helical shapes which is essential for their biological function as cell “propeller”. The co-existence of two conformational states for flagellin within the filament is believed to be responsible for the helical shapes by producing local misfit which results in curvature and twist. In this paper, we present a coarse-grained description with an elastic energy functional for the filament derived from its microscopic structure. By minimising this functional we can answer the question of spatial distribution of flagellin states which is crucial for the observed coupling of curvature and twist.

## 1 Introduction

Bacteria such as *Escherichia coli* and *Salmonella typhimurium* use rotating flagella to swim. Each flagellum consists of a  $\sim 3\mu\text{m}$  long filament coiled into a helix which is connected at one end to a nanomotor embedded into the cell membrane [1, 2]. The filament shows an ability for *polymorphism* allowing for several stable helical shape states with different curvature and twist. Switching between these distinct helical states may be caused by changes in *pH*, ionic strength or applied torsional load [3].

Polymorphism plays a central role for cell motility which is characterised by switching back and forth between helical states of opposite chirality in adaptive intervals  $\sim 1\text{s}$  corresponding to the run and tumble mode of motion [4, 5].

**Outline.** In Section 1.1, we present the microscopic details of the filament that will be cast in our model. Then we discuss the classic approach by Calladine superimposing two separate models for curvature and twist (1.2-1.4) and a recent

---

<sup>1</sup>benjamin.friedrich@mis.mpg.de

model by Srigiriraju and Powers which lacks curvature-twist-coupling. In Section 2, we extend Calladine's model by formulating an elastic energy functional for the filament. Minimisation of this functional leads to a multi-state control problem, which we study in Section 3, to answer the question of helical shapes and the spatial distribution of flagellin states.

## 1.1 The microscopic structure of the filament

In a cross-section of the filament, one distinguishes high density regions at radii  $25\text{\AA}$  and  $r := 45\text{\AA}$ , referred to as *inner* and *outer tube* [3, 1]. Chemically, the filament is a polymer consisting of  $\sim 10^4$  copies of the protein flagellin [1, 2]. Each flagellin has a domain in the inner as well as in the outer tube, roughly aligned in the radial direction as pictured in Fig. 1.

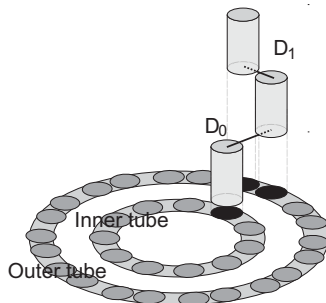


Figure 1: Position of flagellin in the filament

In both the inner and in the outer tube, the respective domains form a two-dimensional lattice as shown in Fig. 2, with each domain represented by a reference dot [3].

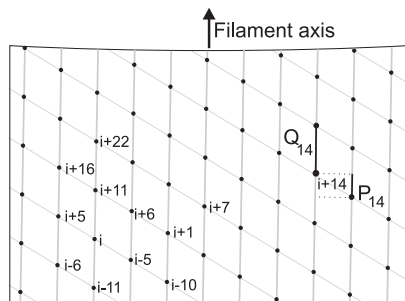


Figure 2: 2D-lattice formed by the flagellin units

Note that the labelling of the monomers is chosen for convenience and does not imply that monomer  $i$  is binding to monomer  $i + 1$ . The binding scheme is as follows: In the inner tube, there exist bonds between monomer  $i$  and  $i \pm 5$ ,  $i \pm 6$  and  $i \pm 11$ ; in the outer tube, the bonds are between  $i$  and  $i \pm 5$ ,  $i \pm 11$  plus a minor bond to  $i \pm 16$  [3, 1, 6].

All monomers in the residue class  $[2i] \in \mathbb{Z}/11\mathbb{Z}$  modulo 11 are referred to as the  $i^{\text{th}}$  *protofilament*.






crossection of filament					
curvature [ $\mu\text{m}^{-1}$ ]	0	1.1	2.7	3.0	0
twist [ $\text{rad } \mu\text{m}^{-1}$ ]	-5.6	-2.1	+1.8	+3.9	13.5
name	<i>R-straight</i>	<i>normal</i>	<i>semi-coiled</i>	<i>curly-1</i>	<i>L-straight</i>

Table 1: Distinct helical states of flagellar filament ( $R$ =black,  $L$ =white)

**Microscopic variables:** We introduce microscopic variables for the outer tube lattice (cf. Fig. 2): (a) the axial spacing  $Q_i$  between the successive flagellins  $i$  and  $i + 11$  within protofilament  $[2i]$  and (b) the axial offset  $P_i$  between the flagellins  $i$  and  $i - 5$  in the neighbouring protofilaments  $[2i]$  and  $[2i+1]$ .

It is convenient to normalise  $q_i := Q_i/Q_{\text{ref}}$  and  $p_i := P_i + \frac{5}{11}Q_{\text{ref}}$ , where  $Q_{\text{ref}}$  is the axial spacing in the unstrained inner tube lattice. In the coarse-grained description to be studied, we will use continuous variables  $q_{[2i]}(s)$  and  $p_{[2i]}(s)$  depending on a length parameter  $s$  parametrising the filament.

**The conformational switch:** One distinguishes two conformational states of flagellin:  $R$  and  $L$  [7], which are believed to result from a conformational switch in the domain  $D1$  [8].

Table 1.1 displays curvature and twist for various polymorphic states together with the assumed spatial distribution of flagellin states (all flagellins in a single protofilament are either in state  $R$  (black) or  $L$  (white)) [3].

Using the mutants *R-straight* and *L-straight*, Yamashita et al. [3] measured the axial spacing  $Q$  as well as the axial offset  $P$  for each of the two states with results as follows

$$Q_R = 51.9 \text{ \AA}, P_R = -24.6 \text{ \AA} \quad \text{and} \quad Q_L = 52.7 \text{ \AA}, P_L = -22.0 \text{ \AA}.$$

One might say that, when switching from  $R$  to  $L$ , a flagellin  $i$  becomes  $0.8 \text{ \AA}$  longer and slides down by  $2.6 \text{ \AA}$  relative to its neighbour flagellin  $i - 5$ .

In a normal filament there will be mixed phases; thus the monomers cannot attain their relaxed geometry and the resulting pre-stress deforms the filament-tube, i.e. it becomes slightly twisted and curved.

## 1.2 Calladine's model for curvature

The first model explaining curvature was given by Calladine [9, 10, 11], supposing

**Calladine's rule:** *In a single protofilament  $[2i]$ , all flagellins are in the same state, say  $\chi_i \in \{L, R\}$  for  $i = 1, \dots, 11$ .*

Calladine then models an infinitesimal section of the filament as two rigid disks of radius  $r$  connected by 11 Hookean springs, assuming that the protofilaments are equally spaced around the circumference of the disks with spring rest length  $q_R$  or  $q_L$  according to  $\chi_i$  (cf. Fig. 3). Let  $q_i$  denote the actual length of the  $i^{\text{th}}$  spring.

In order to minimise the spring energy of this configuration  $E = \sum_{i=1}^{11} \frac{k}{2} (q_i - q_{\chi_i})^2$ , the two disks will be tilted, resulting in local curvature, if the number of  $L$ -

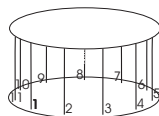


Figure 3: Calladine's spring model

protofilaments differs from 0 or 11. Furthermore, it is energetically favourable to group L-protofilaments together, i.e. minimise  $\#\{i|\chi_i \neq \chi_{i+1}\}$ . Assume that  $\chi_i = L$  for  $i = 1, \dots, l$ , and  $= R$  otherwise. Taking into account the symmetry of the assembly, the length  $q_i$  of the  $i^{\text{th}}$  spring will be  $q_i = a + b \cos \frac{2\pi}{11} \left(i - \frac{l+1}{2}\right)$ , for some  $a, b$ . A short calculation using trigonometric identities yields the minimising values  $a^{\text{opt}} = \frac{1}{11}(lq_L + (11-l)q_R)$  and  $b^{\text{opt}} = \frac{2}{11} \frac{\sin \frac{\#L\pi}{11}}{\sin \frac{\pi}{11}} (q_L - q_R)$ . These values determine the curvature  $k$  of the filament  $\frac{a^{\text{opt}} - b^{\text{opt}}}{a^{\text{opt}}} = \frac{2\pi(1/k - r)}{2\pi 1/k} = 1 - rk$ .

### 1.3 Lattice-rotation-model for twist

A separate model is needed for twist, which is best explained geometrically [12]. Parallel alignment of 11+1 protofilaments (with given offset between neighbouring protofilaments) yields a strip of lattice as in Fig. 4.

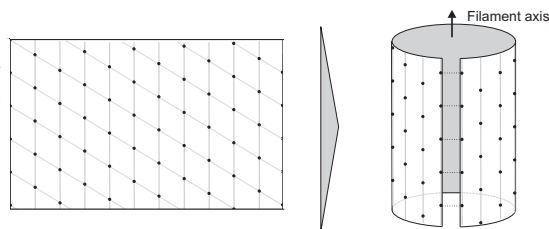


Figure 4: Gluing a strip of lattice into a tube

If the outer rims match, this strip can be closed to a tubular lattice by identifying the two outer protofilaments,

In case there is a mismatch  $p$ , we have to rotate the strip of lattice by an angle  $\theta = \arctan \frac{p}{2\pi r}$  before gluing, to obtain a twisted tube with twist  $\frac{1}{r} \sin \theta$ , as in Fig. 5.

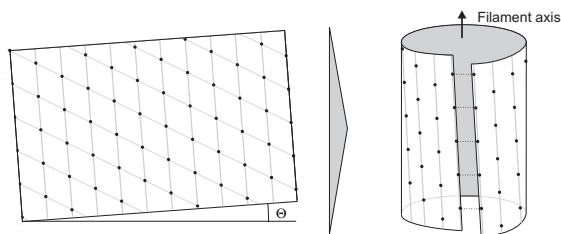


Figure 5: Gluing a rotated strip of lattice into a twisted tube

If the  $i^{\text{th}}$  protofilament switches from state  $R$  to  $L$ , its offset relative to the  $(i+1)^{\text{th}}$  protofilament will change by  $p_L - p_R$ , and thus the twist  $k_3$  of the filament will change by approximately  $\frac{p_L - p_R}{2\pi r^2}$ .

## 1.4 Discussion of the classical approach

Approximately, one can superimpose the predictions of both Calladine's and the lattice rotation model to obtain theoretical values for the helix parameters of the different polymorphic states, in good agreement with experimental data [4, 9]. However, it is not clear why the models do not interfere. Also, Calladine's rule remains unexplained.

## 1.5 Alternative approaches

Hasegawa et al. [13] proposed a modification of Asakura's  $L$ -and- $R$ -state hypothesis in that no distinct conformational states, but instead alternate pairs of binding sites  $(A_1, A_2)$  and  $(B_1, B_2)$  exist at flagellin  $i$ , each of which can form the  $-5$ -bond to a pair  $(C_1, C_2)$  of binding sites at flagellin  $i - 5$ . A difference in the axial offset between the two binding points for the  $A$  and the  $B$ -pair is said to compress flagellin  $i$  by  $0.8\text{\AA}$  when the  $A$ -pair is used, thus leading to a coupling of axial offset and axial spacing. However, when the  $A$ -pair is used, flagellin  $i - 5$  becomes stretched, making it questionable whether the right coupling arises from this theory.

Recently, Srigriraju and Powers [14] proposed a continuum model for bacterial flagella using double-well potentials for the axial spacing variables. In this model Calladine's rule is forced by an explicit phase boundary penalization. Their model can explain the response of the filament to torsional load but lacks the twist-curvature coupling implied by the conformational switch.

## 2 Mesoscopic model

We will employ a semi-continuous approach, modelling the protofilaments as space curves to set up an elastic energy functional  $E$  for the filament exhibiting twist-curvature-coupling.

**Variables.** Let us consider the back-bone of the flagellum  $x(s) \in \mathbb{R}^3$  parametrised by arc-length  $s$  together with a vector field  $e_1(s) \in \mathbb{R}^3$  perpendicular to  $e_3(s) := x'(s)$  and pointing towards the 11<sup>th</sup> protofilament. A prime will always denote differentiation w.r.t.  $s$ . Setting  $e_2(s) := e_3(s) \times e_1(s)$  completes a *material frame* for  $x(s)$  [15, 16]. Using  $\frac{1}{2}\langle e_i, e'_i \rangle = \frac{d}{ds}|e_i|^2 = 0$ , one shows  $e'_i(s) = \underline{k}(s) \times e_i(s)$  for a uniquely determined  $\underline{k} := (k_1, k_2, k_3) : [0, 1] \rightarrow \mathbb{R}^3$ . The case  $\underline{k} = \text{const.}$  corresponds to a perfect helix  $x$  with curvature  $k = \sqrt{k_1^2 + k_2^2}$  and twist  $k_3$ . The physically sound range for  $|k_3|$  is  $|k_3| \ll \frac{1}{r}$ ; for  $k$  it is  $k < \frac{1}{R} \approx 80\mu\text{m}^{-1}$ , where  $R$  is the radius of injectivity of the filament. Note that up to rotations and translations, we can recover the space curve  $x$  from  $\underline{k}$ .

We assume fixed radial distance  $r$  between protofilaments and back-bone, as well as fixed angular spacing  $\frac{2\pi}{11}$  between laterally-adjacent protofilaments. This already determines the protofilaments as abstract space curves, but not their parametrisation. This will be specified by variables  $s_i(t)$ , the  $i^{\text{th}}$  protofilament being given as

$$x_i(t) := x(s_i(t)) + \alpha_i e_1(s_i(t)) + \beta_i e_2(s_i(t)), \text{ where } \alpha_i := r \cos \frac{2\pi i}{11}, \beta_i := r \sin \frac{2\pi i}{11},$$

where  $t$  is a material parameterization of the protofilament. The  $s_i$  have the physical meaning of describing axial sliding and axial stretching of protofilaments and must satisfy  $s'_i > 0$ . The relaxed state corresponds to  $s'_i = 1$ , whereas  $s'_i < 1$  corresponds to compression and  $s'_i > 1$  to stretching of the  $i^{\text{th}}$  protofilament.

Furthermore, we will consider characteristic state functions  $\chi_i(s) \in \{L, R\}$ ,  $i = 1, \dots, 11$ , specifying the state of the flagellin at position  $x_i(s_i^{-1}(s))$  in the  $i^{\text{th}}$  protofilament.

We will study a bulk section of the filament  $s \in \mathbb{I} := (0, 1)$ , neglecting boundary effects at both ends.

**Linearization.** For the axial spacing  $q_i$ , we have (using  $r \ll 1$ , the boundedness of  $k_1, k_2, rk_3$  and  $s'_i \approx 1$ )

$$q_i = \left| \frac{d}{dt} x_i(t) \right| = |e_3 - \alpha_i k_2 e_3 + \alpha_i k_1 e_2 + \beta_i k_1 e_3 - \beta_i k_3 e_1| s'_i(t) \approx s'_i - \alpha_i k_2 + \beta_i k_1.$$

In order to express the axial offset  $p_i$  between neighboring protofilaments, we consider lateral bonds connecting the  $i^{\text{th}}$  and the  $(i+1)^{\text{th}}$  protofilaments which lie in the outer tube and are perpendicular to the two protofilaments. According to the lattice-rotation-model, (the space curve for) the lateral bond starting at  $x_i(s_i^{-1}(s))$  will be given to first-order by

$$y_{i,i+1}(u) = x(s(u)) + r \cos \frac{2\pi(i+u)}{11} e_1(s(u)) + r \sin \frac{2\pi(i+u)}{11} e_2(s(u)),$$

$$\text{where } s(u) = s - \gamma k_3 u,$$

with  $u \in [0, 1]$ ,  $\gamma := \frac{2\pi r^2}{11}$ . Note that  $\langle \frac{d}{dt} x_i(t) |_{t=s_i^{-1}(s)}, \frac{d}{du} y_{i,i+1}(u) |_{u=0} \rangle = 0 + o(r^2)$ . Thus the axial offset between the  $i^{\text{th}}$  and the  $(i+1)^{\text{th}}$  protofilament at arc-length position  $s$  is (using  $s'_i \approx 1$  and  $\gamma k_3 \ll 1$ )

$$p_i(s) = s_{i+1}^{-1}(s - \gamma k_3) - s_i^{-1}(s) \approx s_i(s) - s_{i+1}(s) + \gamma k_3.$$

Integration along protofilaments will be replaced by integration w.r.t.  $ds$ , this being permissible since  $s'_i \approx 1$ .

**Potentials.** The elastic energy  $E$  of the filament will consist of parts coming from the inner and the outer tube plus a term  $E_k$  which penalises distortion of the protofilaments due to curvature

$$E = E_{\text{IT}} + E_{\text{OT}} + E_k = \int W_{\text{IT}} + W_{\text{OT}} + W_k ds.$$

The energy density  $W_{\text{IT}}$  amounts to an axial strain response, thus depending on  $\bar{s}'$ ,  $\bar{s} := \frac{1}{11} \sum_{i=1}^{11} s'_i(s)$ , with a local minimum at  $q_{\text{IT}} = 1$ . We assume  $W_{\text{IT}} = \mu(\bar{s}' - 1)^2$ . Since the protein assembly of the filament is held together only by local bonds, we expect  $W_{\text{OT}}$  to be a sum  $W_{\text{OT}}(\{p_i\}, \{q_i\}, \{\chi_i\}) = \sum_{i=1}^{11} w_{\text{OT}}(p_i(s), q_i(s), \chi_i(s))$ . Little is known about  $w_{\text{OT}}$ , except its non-convexity with distinct local minima at  $(p_R, q_R, R)$  and  $(p_L, q_L, L)$ . Thus, we make a quadratic expansion  $w_{\text{OT}}(p, q, S) = w_p(p, S) + w_q(q, S)$  with  $w_p(p, S) = \lambda_1(p - p_S)^2$  and  $w_q(q, S) = \lambda_2(q - q_S)^2$ . We normalise  $\lambda_2 = 1$  and write  $\lambda := \lambda_1$ .

Finally,  $W_k = \varepsilon(k_1^2 + k_2^2)$  to second order.



**A coupled control problem.** Thus we are led to consider the following control problem (\*).

---

backbone	$k_1, k_2, k_3 \in L^2(\mathbb{I}), \quad \mathbb{I} := (0, 1)$
states	$\chi_1, \dots, \chi_{11} : \mathbb{I} \rightarrow \mathbb{S} := \{R, L\}$
axial shift	$s_1, \dots, s_{11} \in H^1(\mathbb{I})$
constants	$\alpha_i := r \cos \frac{2\pi i}{11}, \beta_i := r \sin \frac{2\pi i}{11}, \gamma := \frac{2\pi r^2}{11}, \mu, \lambda, \varepsilon > 0$ $p : \mathbb{S} \rightarrow \mathbb{R}, \quad p_i^* := p \circ \chi_i \quad \text{and} \quad q : \mathbb{S} \rightarrow \mathbb{R}, \quad q_i^* := q \circ \chi_i$
axial offset	$p_i := t_i - t_{i+1} + \gamma k_3, \quad \text{where} \quad \bar{s} := \frac{1}{11} \sum_{i=1}^{11} s_i, \quad t_i := s_i - \bar{s}$
axial strain	$q_i := \bar{s}' + t_i' - \alpha_i k_2 + \beta_i k_1$
energy	$E(\underline{k}, \underline{s}, \underline{\chi}) := \int_{\mathbb{I}} W_{IT} + W_p + W_q + W_k ds$ $= \int_{\mathbb{I}} \mu(\bar{s}' - 1)^2 + \lambda \sum_{i=1}^{11} (p_i - p_i^*)^2 + \sum_{i=1}^{11} (q_i - q_i^*)^2 + \varepsilon(k_1^2 + k_2^2) ds$

---

### 3 Analysis of the model

Assuming the filament to be in an equilibrium state minimising  $E$ , we can address the question of spatial distribution of flagellin states and ask for helical shapes.

#### 3.1 Calladine's rule

We can prove Calladine's rule in the limiting case of large  $\lambda$ .

**Theorem 1.** *There exists a constant  $C = C(p, q)$  such that for all  $\lambda > C$  the control problem (\*) admits minimiser  $(\underline{k}^{\text{opt}}, s_i^{\text{opt}}, \chi_i^{\text{opt}})$ , all of which satisfy  $\chi_i^{\text{opt}}(s) \equiv \text{const}$ . Moreover, for fixed and constant  $\chi_i$ , the minimiser is unique.*

The proof consists of several lemmas whose proofs can be found in the appendix. First let us present the main idea. For large  $\lambda$ ,  $p_i(s)$  will stay in an  $\varepsilon$ -tube of  $p(S_i)$  for an appropriate  $S_i \in \mathbb{S}$ , if  $E$  is less than a certain constant. Next, for  $C^1$ -candidates  $s_i$  with  $\chi_i$  chosen optimally, each jump of  $\chi_i(s)$  will cost at least an energy amount of  $\tilde{\varepsilon} > 0$ . Applying this argument to a minimising sequence rules out the possibility of convergence to non-trivial Young measures. So we need not convexify the integrand in (\*) at any point in the proof. However, we will not work with the original functional (\*) directly, but with a transformed problem (1) obtained by first eliminating those variables whose derivatives do not appear in the functional, and then applying a Fourier transform.

For given  $t_i, \chi_i$ , we can eliminate  $k_1, k_2, k_3, u := \bar{s}'$  from the functional. First we define shorthand notation  $d_i := t_i' - (q_i^* - \bar{q}^*)$ ,  $\tilde{\mu} := \frac{\mu}{11+\mu}$ ,  $\nu := \frac{2}{11+2\varepsilon/r^2}$ ,  $\bar{p}^* := \sum_{i=1}^{11} p_i^*/11$ , and  $\bar{q}^* := \sum_{i=1}^{11} q_i^*/11$ .

**Lemma 2 (Elimination of variables).** *We have*

$$\begin{aligned} \tilde{W}(\{t_i\}, \{\chi_i\}) &:= \min_{k_1, k_2, k_3, u} W(\underline{k}, \{s_i\}, \{\chi_i\}) \\ &= 11\tilde{\mu}(\bar{q}^* - 1)^2 + \lambda \sum_{i=1}^{11} (t_i - t_{i+1} + \bar{p}^* - p_i^*)^2 + \\ &\quad \sum_{i=1}^{11} d_i^2 - \nu \sum_{i,j=1}^{11} d_i d_j \cos \frac{2\pi}{11}(j - i). \end{aligned}$$

The minimum is attained for  $k_1^{\text{opt}} = -\nu/r^2 \sum_{i=1}^{11} \beta_i d_i$ ,  $k_2^{\text{opt}} = \nu/r^2 \sum_{i=1}^{11} \alpha_i d_i$ ,  $k_3^{\text{opt}} = \bar{p}^*/\gamma$ , and  $\bar{s}'^{\text{opt}} = \frac{\mu+11\bar{q}^*}{\mu+11}$  for given functions  $\chi_i$ .

Next we can decouple the  $t_i$  in  $\tilde{W}$  by using discrete Fourier transform w.r.t.  $i$ .

**Definition 1 (Fourier transform).** For any 11-tuple  $c_1, \dots, c_{11}$  we denote their Fourier transform as

$$\hat{c}_n := \sum_{m=1}^{11} \frac{\langle n, m \rangle}{\sqrt{11}} c_m, \quad n = 1, \dots, 11, \quad \text{where } \langle n, m \rangle = \exp \frac{2\pi i}{11} n \cdot m.$$

Note  $c_m = \sum_{n=1}^{11} \frac{\langle -n, m \rangle}{\sqrt{11}} \hat{c}_n$ .

**Lemma 3 (Fourier transform).** By using the Fourier transforms  $\hat{t}_i$  of  $t_i$ , we can express  $\tilde{W}$  as follows

$$\tilde{W}(\underline{\hat{t}}, \underline{\chi}) = \tilde{\mu}(\hat{q}_0^* - \sqrt{11})^2 + 2 \sum_{k=1}^5 \lambda |(1 - \langle -k, 1 \rangle) \hat{t}_k - \hat{p}_k^*|^2 + 2 \sum_{k=1}^5 |\hat{t}_k - \hat{q}_k^*|^2 - 11\nu |\hat{t}_1 - \hat{q}_1^*|^2,$$

or by defining new variables  $f_k = \text{Re } \hat{t}_k$ ,  $f_{k+5} = \text{Im } \hat{t}_k$ ,  $k = 1, \dots, 5$  as:

$$\tilde{W}(\underline{f}, \underline{\chi}) = \tilde{\mu}(\hat{q}_0^* - \sqrt{11})^2 + \sum_{k=1}^{10} 2\lambda_k (f_k - \tilde{p}_k^*)^2 + 2\nu_k (f'_k - \tilde{q}_k^*)^2$$

where for  $k = 1, \dots, 5$  we set  $\lambda_k = \lambda_{k+5} := \lambda |1 - \langle -k, 1 \rangle|^2$ ,  $\tilde{p}_k^* := \text{Re } \hat{p}_k^* (1 - \langle -k, 1 \rangle)^{-1}$ ,  $\tilde{p}_{k+5}^* := \text{Im } \hat{p}_k^* (1 - \langle -k, 1 \rangle)^{-1}$ ,  $\tilde{q}_k^* := \text{Re } \hat{q}_k^*$ ,  $\tilde{q}_{k+5}^* := \text{Im } \hat{q}_k^*$ ,  $\nu_k = \nu_{k+5} := \varepsilon\nu/r^2$  if  $k = 1$  and  $= 1$  else.

**A simple control problem.** Thus we have transformed the original control problem (\*) into a decoupled sum of simple control problems of the form (with  $n = 2^{11}$ )

$$E(f, \chi) := \int_{\mathbb{I}} \lambda^2 (f - p^*)^2 + (f' - q^*)^2 \rightarrow \min, \quad (1)$$

where  $\mathbb{I} := (0, 1)$ ,  $\mathbb{S} := \{0, \dots, n-1\}$ , and  $p, q : \mathbb{S} \rightarrow \mathbb{R}$  are given functions, and where variation is taken over

$$\begin{aligned} \chi &: \mathbb{I} \rightarrow \mathbb{S}, \text{ required to be left-sided continuous, and} \\ f &: \mathbb{I} \rightarrow \mathbb{R} \text{ with } f \in H^1(\mathbb{I}). \end{aligned}$$

We have used the short-hand notation  $p^* := p \circ \chi$  and  $q^* := q \circ \chi$ .

By Morrey's lemma, the candidate  $f$  is continuous. Thus the case  $\lambda = \infty$  corresponds to  $\chi \equiv \text{const}$  (i.e. selection of a single state) for all  $(f, \chi)$  with finite energy  $E$ . On the other hand, for  $\lambda = 0$ , we can get minimising sequences  $(f_n, \chi_n)$  converging to non-trivial Young-measures [17]. Which behaviour arises for  $0 < \lambda < \infty$ , is a question of theoretical interest. We show that  $\lambda \gg 0$  gives  $\chi \equiv \text{const}$  as well.

**The case of a single state:** For  $n = 1$  we have an ordinary variational problem for which the Euler-Lagrange equation reads

$$\lambda^2(f - p) = f''. \quad (2)$$

From the standard theory [18, 19], we know that a minimiser  $f$  will be a weak solution of (2). Furthermore, basic regularity theory gives  $f \in C^\infty$ , hence  $f$  will be a strong solution of (2).

A straightforward calculation shows that the general solution of (2) is given by

$$f(x) = p + c_1 \cosh(\lambda x) - c_2 \cosh(\lambda(x - 1)).$$

The choice  $c_1 = c_2 = \frac{q}{\lambda \sinh(\lambda)}$  minimises  $E(f)$  to  $E(f^{\text{opt}}) = q^2 \left(1 - \frac{2}{\lambda} \tanh\left(\frac{\lambda}{2}\right)\right)$ .

**The case  $n > 1$  with  $\lambda$  large:** By Lemma 3, the following proposition proves the Theorem. Note that the condition of the proposition can easily be verified by a numerical check.

**Proposition 4.** *Assume  $p$  and  $q$  to be injective. Then there exists a constant  $C := C(p, q)$ , such that for all  $\lambda > C$  the control problem (1) admits minimiser  $(f, \chi)$ , all of which satisfy  $\chi \equiv \text{const}$ . For fixed, constant  $\chi$ , the minimiser is unique.*

A key ingredient in the proof of the proposition is the following lemma.

**Lemma 5.** *Let  $(f, \chi)$  be such that  $E(f, \chi) < Q^2$ , where  $Q := \max_{S \in \mathbb{S}} |q(S)|$ . Then there exists an  $S \in \mathbb{S}$  such that  $|f - p(S)| \leq 2\varepsilon$  in  $\mathbb{I}$ , where  $\varepsilon := Q \max\{1/\lambda, \sqrt{2/\lambda}, \sqrt[3]{2/\lambda^2}\}$ .*

## 3.2 Coexistence of phases

If the axial spacing  $q_{\text{IT}} = 1$  in the inner tube does not match one of the preferred values for the axial spacing in the outer tube,  $q_R$  nor  $q_L$ , mismatch will arise between the inner tube and the outer tube in a pure phase state, i.e. *R-straight* or *L-straight*, thus possibly making a phase mix energetically favourable.

To illustrate the phenomenon, we consider the limit  $\lambda = \infty$ ,  $\varepsilon = 0$ , which forces the constraint  $\hat{t}_k \equiv \hat{p}_k^*$ ,  $\hat{t}'_k = 0$ . Thus the energy simplifies to

$$E = \tilde{\mu}(\hat{q}_0^* - \sqrt{11})^2 + 2 \sum_{k=2}^5 |\hat{q}_k^*|^2.$$

Once we specify  $\bar{q} := \frac{1}{2}(q_L + q_R)$ , we can easily determine  $\chi^{\text{opt}}$  numerically. For  $\bar{q}$  close to  $q_{\text{IT}} = 1$  the number of L-protofilaments in the optimal configuration will be different from 0 or 11, if the stiffness of the inner tube  $\mu$  is not too small (cf. Fig. 6). In this parameter region filaments will be helically coiled.

Figure 6 does not show parameter regions for the *normal* or *semi-coiled* helical state (cf. Table 1.1) which are typical for the wild-type. This deficiency might be due to the use of simple, quadratic potentials. Recent experiments suggest, that the strain-stress-response of  $\alpha$ -helices (the most-common motif in flagellin [8, 6]) lead to 4<sup>th</sup>-order potentials instead [20]. If we use  $w_q(q, S) = (q - q(S))^4$  in the energy functional, we get a modified picture with more helical states (not shown).

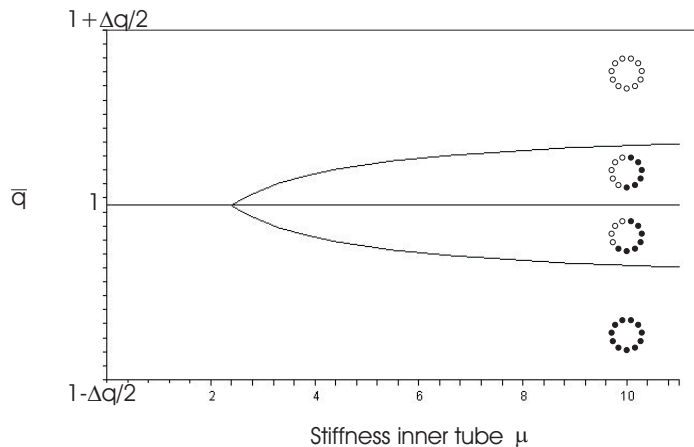


Figure 6: Coexistence of Phases

### 3.3 Connection with the classic approach

The limit  $\lambda = \infty$ ,  $\varepsilon = \mu = 0$  with  $\chi$  prescribed recovers the combination of Calladine's model and the lattice-rotation-model yielding the curvature and twist values reported in the literature (cf. e.g. [3]).

## 4 Discussion

Using an elasticity functional for the bacterial flagellar filament, we have shown rigorously that a strong interaction between laterally adjacent protofilaments can force Calladine's rule, i.e. that each of the filament's protofilaments is in a single state. Figuratively, our argument can be put as follows: If, on a protofilament, L-state and R-state regions meet, these regions will correspond to different values for the preferred offset to the neighbouring protofilament and a mismatch arises, making such a configuration energetically unfavourable. Once Calladine's rule has been established, we can deduce helical shapes for the filament.

## 5 Appendix

*Proof of Lemma 2.* The proof is straight-forward using standard calculus and trigonometric identities.  $\square$

*Proof of Lemma 3.* The proof follows immediately from the following list of identities

**Linearity:**  $(\alpha c_m + \beta d_m)^\wedge = \alpha \hat{c}_m + \beta \hat{d}_m$

**Isometry:**  $\sum_{m=1}^{11} c_m^2 = \sum_{n=1}^{11} |\hat{c}_n|^2$

**Constants:**  $\sum_{m=1}^{11} (c_m - d)^2 = (\hat{c}_0 - \sqrt{11}d)^2 + \sum_{n=1}^{10} |\hat{c}_n|^2$

**Phase shift:**  $\sum_{m=1}^{11} (c_m - d_{m+1})^2 = \sum_{n=1}^{11} |\hat{c}_n - \langle -n, 1 \rangle \hat{d}_n|^2$

1<sup>st</sup> **mode:**  $\sum_{m,n=1}^{11} \cos \frac{2\pi}{11}(n-m)c_m c_n = 11|\hat{c}_1|^2$

□

*Proof of Proposition 4.* Consider a minimising sequence  $\{(f_n, \chi_n)\}$  such that  $E(f_n, \chi_n) \rightarrow \inf E$ . We may assume w.l.o.g. that all  $f_n \in C^1(\mathbb{I})$ . and that  $E(f_n, \chi_n) = \inf_{\phi} E(f_n, \phi)$ . (Since  $f \in C^1$ , the infimum is attained for a  $\chi_n$  having only a finite number of jumps.)

If none of the  $\chi_n$  jumps, we may assume  $\chi_n \equiv \text{const}$ , by restricting to a subsequence (not relabeled). Then the assertion follows from the general theory for convex problems [18, 19].

Therefore, we may assume w.l.o.g. that each  $\chi_n$  jumps at least once. Suppose we could prove the following for some  $\tilde{\varepsilon} > 0$  independent from  $n$ :

$$\forall n \exists (\tilde{f}_n, \tilde{\chi}_n) : E(\tilde{f}_n, \tilde{\chi}_n) + \tilde{\varepsilon} \leq E(f_n, \chi_n), \quad (3)$$

where the number of jumps of  $\tilde{\chi}_n$  is less than the one of  $\chi_n$ .

This will contradict the minimising sequence property of  $(f_n, \chi_n)$ .

In the following, we will prove (3). For simplicity, we drop the subscript  $n$ .

By Lemma 5, we know  $|f - p(S_1)| \leq 2\varepsilon$  for some  $S_1 \in \mathbb{S}$  with  $\varepsilon = c_1 \lambda^{-2/3}$  for  $\lambda > \Lambda_1$  where here and in the following we use  $c$  and  $\Lambda$  for positive constants depending only on  $p$  and  $q$ .

We choose  $a, b \in \bar{\mathbb{I}}$  maximal such that  $\chi(s) = S_1$  in  $(0, a]$  and  $\chi(s) = S_2 \neq S_1$  in  $(a, b]$  for some  $S_2 \in \mathbb{S}$  (possibly  $a = 0$ ).

We define shorthand notation  $p_i := p(S_i)$ ,  $q_i := q(S_i)$ ,  $i = 1, 2$ ,  $p_{21} := p_2 - p_1$ ,  $\bar{p} := \frac{1}{2}(p_1 + p_2)$ ,  $q_{21} := q_2 - q_1$ ,  $\bar{q} := \frac{1}{2}(q_1 + q_2)$ ,  $\delta := b - a > 0$ ,  $h := f(b) - f(a) - q_1 \delta$ , as well as  $(\tilde{f}, \tilde{\chi})$

$$\tilde{f}(t) := \begin{cases} f(t) + h & \text{if } t \leq a \\ f(b) + q_1(t - a) & \text{if } a \leq t \leq b, \\ f(t) & \text{if } t \geq b \end{cases}, \quad \tilde{\chi}(t) := \begin{cases} S_1 & \text{if } t \leq b \\ \chi(t) & \text{if } t > b \end{cases}.$$

The assumption  $\chi$  being optimal implies  $q_{21}(f' - \bar{q}) \geq -\lambda^2 p_{21}(f - \bar{p})$  for  $t \in (a, b)$ . We estimate

$$\begin{aligned} 2q_{21}(f(b) - f(a) - \bar{q}\delta) &= 2q_{21} \int_a^b f'(t) - \bar{q} dt \geq -2\lambda^2 p_{21} \int_a^b f(t) - \bar{p} dt \\ &= \lambda^2 \int_a^b p_{21}^2 - 2p_{21}(f(t) - p_1) \geq \lambda^2 (p_{21}^2 - 4\varepsilon|p_{21}|) \delta \end{aligned}$$

This gives us

$$2q_{21}h \geq \lambda^2 (p_{21}^2 - 4\varepsilon|p_{21}|) \delta - 2q_{21}(q_1 - \bar{q}) \delta.$$

Since  $\varepsilon = c_1 \lambda^{-2/3}$ , we thus obtain  $c_2 \lambda^2 < |h|/\delta$  for  $\lambda > \Lambda_2 > \Lambda_1$ . From  $|h| \leq 4\varepsilon + \delta|q_1|$ , we get  $|h| \leq c_4 \lambda^{-2/3}$  for  $\lambda > \Lambda_3 > \Lambda_2$ . Now we are ready to estimate

$$E(\tilde{f}, \tilde{\chi}) - E(f, \chi)$$

$$\begin{aligned} E(\tilde{f}, \tilde{\chi}) - E(f, \chi) &= \int_0^a \lambda^2 (f(t) + h - p_1)^2 - \lambda^2 (f(t) - p_1)^2 dt \\ &\quad + \int_a^b \lambda^2 (f(b) + q_1(t - b) - p_1)^2 - \lambda^2 (f(t) - p_2)^2 - (f'(t) - q_2)^2 dt \\ &\stackrel{\text{Jensen}}{\leq} \lambda^2 (h^2 + 4\varepsilon|h|) + \lambda^2 (2\varepsilon + |q_1|\delta)^2 \delta - \lambda^2 \min\{0, |p_{21}| - 2\varepsilon\}^2 - \frac{(h - q_{21}\delta)^2}{\delta} \\ &\leq (c_5\lambda^{4/3} + c_6\lambda^{-4/3} - c_7\lambda^2)|h| - \tilde{\varepsilon} \leq -\tilde{\varepsilon} \quad \text{for } \lambda > \Lambda_4 > \Lambda_3, \end{aligned}$$

where  $\tilde{\varepsilon} := \lambda^2 \min_{S \neq T} |p(S) - p(T)|^2/4$ .  $\square$

*Proof of Lemma 5.* We distinguish between three cases.

**Case 1: The lemma holds.**

**Case 2: For all  $S \in \mathbb{S}$  it holds  $|f - p(S)| \geq \varepsilon$ .** Then  $E(u, \chi) \geq \lambda^2 \varepsilon^2 \geq Q^2$ , which is a contradiction.

**Case 3: There exist  $S \in \mathbb{S}, t_1, t_2 \in \mathbb{I}$  such that  $|f(t_1) - p(S)| \leq \varepsilon$  and  $|f(t_2) - p(S)| \geq 2\varepsilon$ .** W.l.o.g.  $|f(t) - p(S)| \geq \varepsilon$  for all  $t \in [t_1, t_2]$ . Define  $\delta := |t_2 - t_1|$  and  $\sigma := \frac{f(t_2) - f(t_1)}{t_2 - t_1}$ . Note  $|\sigma| \geq \varepsilon/\delta$ . We set

$$h(\zeta) := \begin{cases} (\zeta + Q)^2 & \text{if } \zeta \leq -Q \\ 0 & \text{if } -Q \leq \zeta \leq Q \\ (\zeta - Q)^2 & \text{if } \zeta \geq Q \end{cases}$$

Now

$$E \geq \lambda^2 \varepsilon^2 \delta + \int_{t_1}^{t_2} h(f') \stackrel{\text{Jensen}}{\geq} \lambda^2 \varepsilon^2 \delta + h(\sigma) \delta.$$

**Case 3.1:  $|\sigma| \geq 2Q$  holds.** We obtain  $E \geq \lambda^2 \varepsilon^2 \delta + \left(\frac{\varepsilon}{2}\right)^2 \delta \geq \lambda^2 \varepsilon^2 \delta + \frac{\varepsilon^2}{4\delta} \geq \frac{\lambda \varepsilon^2}{2} \geq Q^2$ .

**Case 3.2:  $|\sigma| \leq 2Q$  holds.** From  $\delta \geq \frac{\varepsilon}{2Q}$ , we see  $E \geq \frac{\lambda^2 \varepsilon^3}{2Q} \geq Q^2$ .

Since we have ruled out cases 2 and 3, we proved the lemma.  $\square$

## 6 Acknowledgement

I would like to thank Angela Stevens and Stephan Luckhaus for proposing this subject and useful discussions.

## References

- [1] K. Namba and F. Vonderviszt. Molecular architecture of bacterial flagellum. *Quart. Rev. of Biophys.*, 30(1):1–65, 1997.
- [2] H.C. Berg. The rotary motor of bacterial flagella. *Annu. Rev. Biochem.*, 72:19–54, 2003.
- [3] I. Yamashita, K. Hasegawa, H. Suzuki, F. Vonderviszt, Y. Mimori-Kiyosue, and K. Namba. Structure and switching of bacterial flagellar filaments studied by X-ray fiber diffraction. *Nature Struct. Bio.*, 5(2):125–132, 1998.

- [4] L. Turner, W.S. Ryu, and H.C. Berg. Real-time imaging of fluorescent flagellar filaments. *J. of Bacteriol.*, 182(10):2793–2801, 2000.
- [5] D.W. Stroock. Some stochastic processes which arise from a model of the motion of a bacterium. *Z. Wahrscheinlichkeitstheorie verw. Geb.*, 28:305–315, 1974.
- [6] K. Yonekura, S. Maki-Yonekura, and K. Namba. Complete atomic model of the bacterial flagellar filament by electron cryomicroscopy. *Nature*, 424:643–650, 2003.
- [7] S. Asakura. Polymerization of flagellin and polymorphism of flagella. *Adv. Biophys.*, 1:99–155, 1970.
- [8] F.A. Samatey, K. Imada, S. Nagashima, F. Vonderviszt, T. Kumasaka, M. Yamamoto, and K. Namba. Structure of the bacterial flagellar protofilament and implications for a switch for supercoiling. *Nature*, 410:331–337, 2001.
- [9] C.R. Calladine. Design requirements for the construction of bacterial flagella. *J. Theor. Biol.*, 57:469–489, 1976.
- [10] C.R. Calladine. Change of waveform in bacterial flagella: the role of mechanics at the molecular level. *J. Molec. Biol.*, 118:457–479, 1978.
- [11] C.R. Calladine. Construction of bacterial flagellar filaments, and aspects of their conversion to different helical forms. In W.B. Amos and J.G. Duckett, editors, *Prokaryotic and eukaryotic flagella, Proc. 35th Symp. of Soc. Exper. Biol.*, pages 33–51. CUP, 1982.
- [12] J. Howard. *Mechanics of Motor Proteins and the Cytoskeleton*. Sinauer, 2001.
- [13] K. Hasegawa, I. Yamashita, and K. Namba. Quasi- and nonequivalence in the structure of bacterial flagellar filament. *Biophys. J.*, 74:569–575, 1998.
- [14] S.V. Srigiriraju and T.R. Powers. Continuum model for polymorphism of bacterial flagella. *Phys. Rev. Lett.*, 94:248101, 2005.
- [15] R.E. Goldstein, A. Goriely, G. Huber, and C.W. Wolgemuth. Bistable helices. *Phys. Rev. Lett.*, 84:1631–1634, 2000.
- [16] R.L. Bishop. There is more than one way to frame a curve. *Am. Math. Monthly*, 82:246, 1975.
- [17] A. Braides.  *$\Gamma$ -convergence for beginners*. Oxford UP, 2002.
- [18] L.C. Evans. *Partial differential equations*. AMS, 1998.
- [19] B. Dacorogna. *Direct methods in the calculus of variations*. Springer, 1989.
- [20] J. Ireta, J. Neugebauer, M. Scheffler, A. Rojo, and M. Galván. Structural transitions in the polyaniline  $\alpha$ -helix under uniaxial strain. Available online: [w3.rz-berlin.mpg.de/~ireta/member/highlights/pes\\_helix-v5.pdf](http://w3.rz-berlin.mpg.de/~ireta/member/highlights/pes_helix-v5.pdf).